

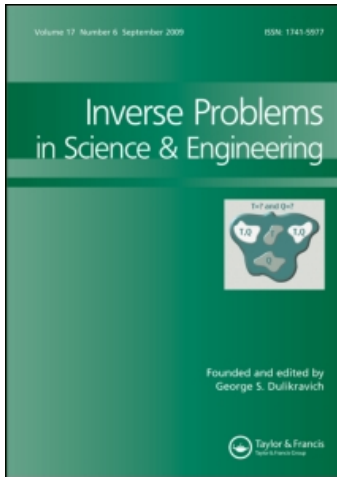
This article was downloaded by: [Gong, Rongfang]

On: 20 March 2010

Access details: Access Details: [subscription number 920021135]

Publisher Taylor & Francis

Informa Ltd Registered in England and Wales Registered Number: 1072954 Registered office: Mortimer House, 37-41 Mortimer Street, London W1T 3JH, UK



Inverse Problems in Science and Engineering

Publication details, including instructions for authors and subscription information:

<http://www.informaworld.com/smpp/title~content=t713643452>

Bioluminescence tomography for media with spatially varying refractive index

R. F. Gong ^a; X. -L. Cheng ^b; W. Han ^c

^a Department of Mathematics, Nanjing University of Aeronautics and Astronautics, Nanjing 210016, P.R. China ^b Department of Mathematics, Zhejiang University, Hangzhou 310027, P.R. China ^c

Department of Mathematics, University of Iowa, Iowa City, IA 52242, USA

Online publication date: 18 March 2010

To cite this Article Gong, R. F., Cheng, X. -L. and Han, W. (2010) 'Bioluminescence tomography for media with spatially varying refractive index', *Inverse Problems in Science and Engineering*, 18: 3, 295 – 312

To link to this Article: DOI: 10.1080/17415970903545132

URL: <http://dx.doi.org/10.1080/17415970903545132>

PLEASE SCROLL DOWN FOR ARTICLE

Full terms and conditions of use: <http://www.informaworld.com/terms-and-conditions-of-access.pdf>

This article may be used for research, teaching and private study purposes. Any substantial or systematic reproduction, re-distribution, re-selling, loan or sub-licensing, systematic supply or distribution in any form to anyone is expressly forbidden.

The publisher does not give any warranty express or implied or make any representation that the contents will be complete or accurate or up to date. The accuracy of any instructions, formulae and drug doses should be independently verified with primary sources. The publisher shall not be liable for any loss, actions, claims, proceedings, demand or costs or damages whatsoever or howsoever caused arising directly or indirectly in connection with or arising out of the use of this material.

Bioluminescence tomography for media with spatially varying refractive index

R.F. Gong^{a*}, X.-L. Cheng^b and W. Han^c

^aDepartment of Mathematics, Nanjing University of Aeronautics and Astronautics, Nanjing 210016, P.R. China; ^bDepartment of Mathematics, Zhejiang University, Hangzhou 310027, P.R. China; ^cDepartment of Mathematics, University of Iowa, Iowa City, IA 52242, USA

(Received 13 February 2009; final version received 4 November 2009)

Biomedical imaging has developed into the level of molecular imaging. Bioluminescence tomography (BLT), as an optical imaging modality, is a rapidly developing new and promising field. So far, much of the theoretical analysis of BLT is based on a diffusion approximation equation for media with constant refractive index. In this article, we study the BLT problem for media with spatially varying refractive index. We introduce a general framework with Tikhonov regularization for this purpose, present its well-posedness and establish the error bounds for its numerical solution by the finite element method. Numerical results are reported on simulations of the BLT problem for media with spatially varying refractive index.

Keywords: bioluminescence tomography; spatially varying refractive index; inverse problem; well-posedness; numerical solution; error estimate

AMS Subject Classifications: 92C55; 34K29; 49K40; 34K28; 65N15

1. Introduction

With the development of science and technology, these years have witnessed the rapid progress in biomedical imaging. Bioluminescent imaging (BLI), as one of the optical imaging modalities, has its own advantages over traditional imaging methods such as computed tomography (CT), positron emission tomography (PET) [1,2], magnetic resonance imaging (MRI) [3,4] as well as their combinations. For instance, compared to PET and MRI, BLI is low in cost. It is particularly attractive for *in vivo* applications because no external excitation source is needed, and thus background noise is low while sensitivity is high. For *in vivo* studies in a big biological object such as human body, BLI is limited to superficial sites owing to the absorption and scattering properties of tissue to light and in this case, PET and MRI are preferred modalities [5].

Bioluminescence tomography (BLT) is a promising BLI because of the possibility of revealing molecular and cellular activity in real time [6,7]. Over the past several years, numerous articles have been devoted to the theoretical analysis and numerical simulations

*Corresponding author. Email: gongrongfang319@yahoo.com.cn

of BLT, (see e.g. [8–16] and references therein). The main objective of BLT is to determine the photon density distribution within small-animals or on the surface of some organs from the light measurement on the boundary. With BLT, a bioluminescent source distribution inside a living small animal can be located and quantified in 3D. Because the transport of light in any entity is subject to both absorption and scattering, the accurate representation of the photon transport in a biological tissue is required. The first step of BLT is to determine the optical properties of tissue and this is the issue of a diffuse optical tomography (DOT) problem. In general, the bioluminescent photon propagation in a tissue can be described accurately by either the radiative transfer equation (RTE) or the Monte Carlo model (MCM) [17]. However, at the moment, neither is computationally feasible. Usually a diffusion approximation of the RTE is employed when the wavelength of light is in the range of around or bigger than 600 nm [18].

In the literature, the BLT is mostly studied based on a diffusion approximation equation to the RTE with constant refractive index of media. In this work, we consider the BLT problem for media with spatially varying refractive index. Consideration of media with spatially inhomogeneous refractive index can be found in [19–25] and [26,27], the DOT problem for such media is studied.

Let $\Omega \subset \mathbb{R}^d$ be a non-empty, open and bounded set with a Lipschitz boundary $\Gamma \triangleq \partial\Omega$ and S^{d-1} the unit sphere in \mathbb{R}^d . In applications, $d=3$. With the diffusion approximation, our BLT problem in spatially varying refractive index media consisting of determining a source function S so that the solution of the following boundary-value problem (BVP):

$$-\operatorname{div}\left[D\left(\nabla - \frac{2\nabla n}{n}\right)u\right] + \mu_a u = S\chi_{\Omega_0} \quad \text{in } \Omega, \tag{1}$$

$$u + 2D\left(\partial_\nu - \frac{2}{n}\partial_\nu n\right)u = 0 \quad \text{on } \Gamma \tag{2}$$

satisfies the measurement condition

$$g = -D\partial_\nu u \quad \text{on } \Gamma_0 \subset \Gamma. \tag{3}$$

Here, Ω_0 and Γ_0 are measurable subsets of Ω and Γ , respectively, both with a positive measure. The symbol χ_{Ω_0} stands for the characteristic function of Ω_0 which takes on the value 1 in Ω_0 and 0 in $\Omega \setminus \Omega_0$. The coefficient $D = [3(\mu_a + \mu'_s)]^{-1}$, μ_a and μ'_s are the absorption and reduced scattering coefficients, and n is the refractive index. We denote $\partial_\nu \cdot$ for the outward normal derivative on Γ . The measured light flux g on Γ_0 is an element in space $L^2(\Gamma_0)$. In applications, it is unrealistic to have measurement on the entire boundary. In this article, we focus on the situation where Γ_0 is a proper subset of Γ .

As in [12], we can show that the pointwise formulation (1)–(3) of the BLT problem is ill-posed. In this article, the BLT problem is studied through a Tikhonov regularization.

We will need some function spaces. For a set G as Ω , Ω_0 or Γ etc., we denote by $W^{m,s}(G)$ the standard Sobolev spaces of degree s and order m with norm $\|\cdot\|_{m,s,G}$, and rewrite them as $L^s(G)$ when $m=0$. Particularly, $H^m(G)$ represents $W^{m,2}(G)$ with corresponding inner product $(\cdot, \cdot)_{m,G}$, norm $\|\cdot\|_{m,G}$ and seminorm $|\cdot|_{m,G}$. Moreover, denote $L^2(\Omega_0)$ by Q . We further denote by c a constant which may have different value in different place.

The structure of this article is as follows. In the next section, we study the BLT problem with a Tikhonov regularization. We address the well-posedness of the regularized BLT problem and explore the limiting behaviours as regularization parameter tends to zero and infinity. In Section 3, we use the finite element method to approximate the regularized BLT problem and obtain some error estimates. We present some numerical examples in the last section.

2. A formulation for BLT with spatially varying refractive index media

By a standard process, we obtain the following weak formulation of the BVP (1)–(2):

$$u \in H^1(\Omega) : \quad a_1(u, v) = (S, v)_{0, \Omega_0} \quad \forall v \in H^1(\Omega), \quad (4)$$

where the bilinear form

$$a_1(u, v) = \int_{\Omega} \left[D \left(\nabla - \frac{2}{n} \nabla n \right) u \cdot \nabla v + \mu_a u v \right] dx + \frac{1}{2} \int_{\Gamma} u v d\sigma \quad u, v \in H^1(\Omega). \quad (5)$$

Let $\Gamma_1 = \Gamma \setminus \Gamma_0$. Since the measurement (3) is available on a proper subset of Γ only, we have $|\Gamma_1| > 0$. Define an inner product $[\cdot, \cdot]$ and the corresponding norm $\|\cdot\|$ over $H^1(\Omega)$ as follows:

$$[u, v] = (\nabla u, \nabla v)_{0, \Omega} + (u, v)_{0, \Gamma}, \quad \|v\| = [v, v]^{1/2} \quad \forall u, v \in H^1(\Omega).$$

It is well-known that the norm $\|\cdot\|$ defined above is equivalent to the norm $\|\cdot\|_{1, \Omega}$.

We will make the following assumption throughout this article:

Assumption (A) Let $0 < b_1 \leq D \leq \mathbf{c}_1$, $\mu_a > 0$, $\|\mu_a\|_{0, \infty} \leq \mathbf{c}_2$, $n \in W^{1, \infty}(\Omega)$, $\| \frac{2}{n} \nabla n \|_{0, \infty} \leq \mathbf{c}_3$, $\|v\|_{0, \Omega} \leq \mathbf{c}_4 \|v\|$, and $\min\{b_1, 1/2\} > \mathbf{c}_1 \mathbf{c}_3 \mathbf{c}_4$.

Under Assumption (A), it is shown in [26] that for each $S \in Q$, the problem (4) admits a unique and stable solution $u \in H^1(\Omega)$.

We comment that it is possible to weaken Assumption (A). In applications, the index function n is nearly piecewise constant, i.e. it is piecewise constant in most parts of Ω except in a small neighbourhood of the interfaces of the sub-regions. In other words, there is a small number $\varepsilon > 0$ such that for a subset Ω_ε of Ω with $|\Omega_\varepsilon| \leq \varepsilon$, $\nabla n = 0$ in $\Omega_1 \triangleq \Omega \setminus \overline{\Omega_\varepsilon}$. Consider the case of one dimension, $d = 1$. By a Sobolev embedding theorem ([28]), there is a constant c_1 such that

$$\|v\|_{0, \infty, \Omega} \leq \tilde{\mathbf{c}} \|v\|_{1, \Omega} \quad \forall v \in H^1(\Omega). \quad (6)$$

Assumption (B) For b_1 , \mathbf{c}_1 , \mathbf{c}_3 , \mathbf{c}_4 and $\tilde{\mathbf{c}}$ given as in Assumption (A) and (6), $\eta = \min\{b_1, \frac{1}{2}\} - \mathbf{c}_1 \mathbf{c}_3 (\mathbf{c}_4 + 1) \tilde{\mathbf{c}} \varepsilon^{1/2} > 0$.

PROPOSITION 2.1 *In the case $d = 1$, under Assumption (B), for each $S \in Q$, the problem (4) admits a unique solution $u \in H^1(\Omega)$ such that*

$$\|u\|_{1, \Omega} \leq c \|S\|_{0, \Omega_0} \quad (7)$$

for some constant $c > 0$, which is independent of S but may depend on the parameters Ω , D , n and μ_a .

Proof We apply the Lax–Milgram lemma [28]; the only major task is to prove the coercivity of the bilinear form $a_1(\cdot, \cdot)$. By using the Hölder inequality, (6) and Schwarz’ inequality, we have

$$\begin{aligned} \left| \int_{\Omega} \frac{2D}{n} u \nabla n \cdot \nabla v \, dx \right| &= \left| \int_{\Omega_\varepsilon} \frac{2D}{n} u \nabla n \cdot \nabla v \, dx \right| \leq c_1 c_3 \int_{\Omega_\varepsilon} |u| |\nabla v| \, dx \\ &\leq c_1 c_3 \|u\|_{0, \infty, \Omega_\varepsilon} \|\nabla v\|_{0, 1, \Omega_\varepsilon} \\ &\leq c_1 c_3 \tilde{c} \|u\|_{1, \Omega} \|\nabla v\|_{0, \Omega_\varepsilon} |\Omega_\varepsilon|^{1/2} \\ &\leq c_1 c_3 (c_4 + 1) \tilde{c} \varepsilon^{1/2} \|u\| \|v\| \quad \forall u, v \in H^1(\Omega). \end{aligned} \tag{8}$$

Hence, from Schwarz’ inequality together with (8), and by noticing $\mu_a \geq 0$ in Ω , we have

$$\begin{aligned} a_1(u, u) &\geq \min \left\{ b_1, \frac{1}{2} \right\} \left(\|u\|_{1, \Omega}^2 + \|u\|_{0, \Gamma}^2 \right) - \left| \int_{\Omega_\varepsilon} \frac{2D}{n} \nabla n u \cdot \nabla u \, dx \right| \\ &\geq \min \left\{ b_1, \frac{1}{2} \right\} \|u\|^2 - c_1 c_3 (c_4 + 1) \tilde{c} \varepsilon^{1/2} \|u\|^2 \\ &= \eta \|u\|^2 \geq c \eta \|u\|_{1, \Omega}^2. \end{aligned} \tag{9}$$

Therefore, we attain the coercivity of the bilinear form $a_1(\cdot, \cdot)$. ■

We note that Assumption (B) is weaker than Assumption (A) for small ε . More delicate arguments are needed to weaken the conditions on data for the coercivity in two/three dimension spaces.

Since the BLT problem in the pointwise form is ill-posed, we will study the BLT problem through a Tikhonov regularization [29–31]. We shall only consider the case where the refractive index is constant near the domain boundary. Consequently, the boundary condition (2) reduces to

$$u + 2D\partial_\nu u = 0 \quad \text{on } \Gamma. \tag{10}$$

Combine (3) and the boundary condition (10) to get

$$u = 2g \quad \text{on } \Gamma_0. \tag{11}$$

From (3), we obtain another mixed boundary condition

$$D\partial_\nu u = -g \quad \text{on } \Gamma_0, \quad u + 2D\partial_\nu u = 0 \quad \text{on } \Gamma_1. \tag{12}$$

We form two boundary value problems: Equation (1) with boundary condition (10) and Equation (1) with boundary condition (12). We then try to minimize the differences between the solutions of these problems with $2g$ on the boundary Γ_0 . In addition to $a_1(\cdot, \cdot)$ defined in (5), let

$$a_2(u, v) = \int_{\Omega} \left[D \left(\nabla - \frac{2}{n} \nabla n \right) u \cdot \nabla v + \mu_a u v \right] dx + \frac{1}{2} \int_{\Gamma_1} u v \, d\sigma \quad \forall u, v \in H^1(\Omega).$$

For any $T \in Q$, denote by $u_1 = u_1(T)$, $u_2 = u_2(T) \in H^1(\Omega)$ the corresponding weak solutions:

$$a_1(u_1, v) = (T, v)_{0, \Omega_0} \quad \forall v \in H^1(\Omega), \tag{13}$$

$$a_2(u_2, v) = -(g, v)_{0, \Gamma_0} + (T, v)_{0, \Omega_0} \quad \forall v \in H^1(\Omega). \tag{14}$$

Under Assumption (A), both problems are uniquely solvable. Moreover, we have the bound

$$\|u_2(T)\|_{1,\Omega} \leq c(\|g\|_{0,\Gamma_0} + \|T\|_{0,\Omega_0}). \quad (15)$$

For $r \in [0, 1]$ and $\alpha \geq 0$, we introduce the following cost functional:

$$J_{r,\alpha}(T) = \frac{r}{2} \|u_1(T) - 2g\|_{0,\Gamma_0}^2 + \frac{1-r}{2} \|u_2(T) - 2g\|_{0,\Gamma_0}^2 + \frac{\alpha}{2} \|T\|_{0,\Omega_0}^2 \quad \forall T \in Q. \quad (16)$$

Then we define a general regularized BLT problem as follows.

Problem 2.2 Find $S_{r,\alpha} \in Q_{ad}$ such that

$$J_{r,\alpha}(S_{r,\alpha}) = \inf_{T \in Q_{ad}} J_{r,\alpha}(T), \quad (17)$$

where Q_{ad} is a convex closed subset of the space Q .

We comment that here we have introduced a family of regularized BLT problems, depending on a parameter $r \in [0, 1]$. The conventional choice for solving the BLT problem is $r = 1$. However, the numerical results in the final section suggest that a proper choice of the parameter r leads to an improvement in the reconstruction accuracy compared to the conventional choice, with only a slight increase in the computational effort since the stiffness matrix and the load vector in the finite element solution of the problem (13) can be used in constructing the finite element system for the problem (14).

By extending the arguments used in [10,12], we can show the following main properties of Problem 2.2.

PROPOSITION 2.3 For any $\alpha > 0$ and $r \in [0, 1]$, Problem 2.2 has a unique solution $S_{r,\alpha} \in Q_{ad}$ which can be characterized by a variational inequality

$$\begin{aligned} & \alpha(S_{r,\alpha}, T - S_{r,\alpha})_{0,\Omega_0} + r(u_1(S_{r,\alpha}) - 2g, u_1(T - S_{r,\alpha}))_{0,\Gamma_0} \\ & + (1-r)(u_2(S_{r,\alpha}) - 2g, u_2(T) - u_2(S_{r,\alpha}))_{0,\Gamma_0} \geq 0 \quad \forall T \in Q_{ad}. \end{aligned} \quad (18)$$

When Q_{ad} is a subspace of Q , the inequality reduces to a variational equality for any $T \in Q_{ad}$

$$\begin{aligned} & \alpha(S_{r,\alpha}, T)_{0,\Omega_0} + r(u_1(S_{r,\alpha}) - 2g, u_1(T))_{0,\Gamma_0} \\ & + (1-r)(u_2(S_{r,\alpha}) - 2g, u_2(T) - u_2(0))_{0,\Gamma_0} = 0. \end{aligned}$$

The solution $S_{r,\alpha}$ depends continuously on the measurement $g \in L^2(\Gamma_0)$, the regularized parameter $\alpha > 0$, coefficients $D \in L^\infty(\Omega)$, $n \in W^{1,\infty}(\Omega)$ and $\mu_\alpha \in L^\infty(\Omega)$.

Assume that $0 \in Q_{ad}$. Then $\|S_{r,\alpha}\|_{0,\Omega_0} \rightarrow 0$ as $\alpha \rightarrow \infty$.

Assume that $S_r \subset Q_{ad}$, the solution set of Problem 2.2 for $\alpha = 0$, is nonempty. Then, $S_{r,\alpha} \rightarrow S_{r,*}$ as $\alpha \rightarrow 0^+$, where $S_{r,*} \in S_r$ satisfies

$$\|S_{r,*}\|_{0,\Omega_0} = \inf_{S \in S_r} \|S\|_{0,\Omega_0}.$$

We also have the following result.

PROPOSITION 2.4 Let $\alpha > 0$. Denote by $S_{0,\alpha}$ and $S_{1,\alpha}$ the unique solutions of Problem 2.2 for $r = 0$ and $r = 1$, respectively. Then $S_{r,\alpha} \rightarrow S_{0,\alpha}$ in Q as $r \rightarrow 0^+$, $S_{r,\alpha} \rightarrow S_{1,\alpha}$ in Q as $r \rightarrow 1^-$.

Proof We only prove the second assertion, i.e. $S_{r,\alpha} \rightarrow S_{1,\alpha}$ in Q as $r \rightarrow 1^-$. The first assertion can be proved similarly. For each parameter α ,

$$J_{r,\alpha}(S_{r,\alpha}) \leq J_{r,\alpha}(S_{1,\alpha}).$$

So the sequence $\{S_{r,\alpha}\}_r$ is bounded, and there is a subsequence denoted again by $\{S_{r,\alpha}\}_r$ and an element $S_{*,\alpha} \in Q$, such that

$$S_{r,\alpha} \rightharpoonup S_{*,\alpha}, \quad \text{in } Q \text{ as } r \rightarrow 1^-.$$

Apparently, $S_{*,\alpha} \in Q_{ad}$. Denote $u_{1,r} = u_1(S_{r,\alpha})$, $u_{2,r} = u_2(S_{r,\alpha})$. Then

$$a_1(u_{1,r}, v) = (S_{r,\alpha}, v)_{0,\Omega_0} \quad \forall v \in H^1(\Omega), \tag{19}$$

$$a_2(u_{2,r}, v) = -(g, v)_{0,\Gamma_0} + (S_{r,\alpha}, v)_{0,\Omega_0} \quad \forall v \in H^1(\Omega). \tag{20}$$

From relations (7) and (15) as well as the boundedness of sequence $\{S_{r,\alpha}\}_r$, we gain the boundedness of sequences $\{\|u_{1,r}\|_{1,\Omega}\}_{r_2}$ and $\{\|u_{2,r}\|_{1,\Omega}\}_{r_2}$. Consequently, resorting to a further subsequence if necessary, there are $u_{1,*}, u_{2,*} \in H^1(\Omega)$ such that

$$u_{1,r} \rightharpoonup u_{1,*}, \quad u_{2,r} \rightharpoonup u_{2,*} \quad \text{in } H^1(\Omega), \text{ as } r \rightarrow 1^-.$$

Particularly, $u_{1,r} \rightharpoonup u_{1,*}$ in $L^2(\Gamma)$ and $u_{2,r} \rightharpoonup u_{2,*}$ in $L^2(\Gamma_1)$, as $r \rightarrow 1^-$. Then pass through $r \rightarrow 1^-$ in (19) and (20) to get

$$\begin{aligned} a_1(u_{1,*}, v) &= (S_{*,\alpha}, v)_{0,\Omega_0} \quad \forall v \in H^1(\Omega), \\ a_2(u_{2,*}, v) &= -(g, v)_{0,\Gamma_0} + (S_{*,\alpha}, v)_{0,\Omega_0} \quad \forall v \in H^1(\Omega). \end{aligned}$$

Hence, $u_{1,*} = u_1(S_{*,\alpha})$ and $u_{2,*} = u_2(S_{*,\alpha})$, that is,

$$u_1(S_{r,\alpha}) \rightharpoonup u_1(S_{*,\alpha}), \quad u_2(S_{r,\alpha}) \rightharpoonup u_2(S_{*,\alpha}) \quad \text{in } H^1(\Omega), \text{ as } r \rightarrow 1^-.$$

Letting $r \rightarrow 1^-$ in (18), we have

$$(u_1(S_{*,\alpha}) - 2g, u_1(T - S_{*,\alpha}))_{0,\Gamma_0} + \alpha(S_{*,\alpha}, T - S_{*,\alpha})_{0,\Omega_0} \geq 0 \quad \forall T \in Q_{ad}, \tag{21}$$

which gives $S_{*,\alpha} = S_{1,\alpha}$ from the uniqueness of the solution of Problem 2.2 for $r = 1$. Therefore, the entire sequence $\{S_{r,\alpha}\}_r$ converges weakly to $S_{1,\alpha}$ as $r \rightarrow 1^-$, from the independence of the choice of subsequences in the arguments above. Strong convergence is shown as follows. Take $T = S_{1,\alpha}$ in (18) and $T = S_{r,\alpha}$ in (21), and add the two resulting inequalities to obtain

$$\begin{aligned} &r \|u_1(S_{r,\alpha} - S_{1,\alpha})\|_{0,\Gamma_0}^2 + \alpha \|S_{r,\alpha} - S_{1,\alpha}\|_{0,\Omega_0}^2 \\ &\leq (1-r)(u_2(S_{r,\alpha}) - 2g, u_2(S_{r,\alpha}) - u_2(S_{1,\alpha}))_{0,\Gamma_0} \rightarrow 0, \text{ as } r \rightarrow 1^-. \end{aligned}$$

We conclude the strong convergence of $\{S_{r,\alpha}\}_r$ to $S_{1,\alpha}$ as $r \rightarrow 1^-$. ■

3. Numerical approximation of BLT

In this section, we consider numerical approximation of Problem 2.2. The standard FEMs are applied to discretize the BLT problem. Let $\{\mathcal{T}_h\}_h$ be a regular family of triangulations over domain $\overline{\Omega}$ with meshsize $h > 0$. For each triangulation $\mathcal{T}_h = \{K\}$, define the linear

finite element space $V^h \triangleq \{v \in C(\overline{\Omega}), v|_K \in \mathcal{P}_1 \forall K \in \mathcal{T}_h\}$. Here \mathcal{P}_k denotes the space of all polynomials of degree $\leq k$. Assume that $\{\mathcal{T}_{0,H}\}_H$ is a regular family of triangulations of $\overline{\Omega}_0$ with meshsize H . Define the space $Q^H = \{T \in Q \mid T|_K \in \mathcal{P}_0(K) \forall K \in \mathcal{T}_{0,H}\}$ and set $Q_{ad}^H = Q^H \cap Q_{ad}$. Let $\Pi^H: Q \rightarrow Q^H$ be an orthogonal projection operator defined by

$$(\Pi^H T, T^H)_{0,\Omega_0} = (T, T^H)_{0,\Omega_0} \quad \forall T \in Q, T^H \in Q^H. \tag{22}$$

Define $u_1^h = u_1^h(T), u_2^h = u_2^h(T) \in V^h$ by

$$\begin{aligned} a_1(u_1^h, v^h) &= (T, v^h)_{0,\Omega_0} \quad \forall v^h \in V^h, \\ a_2(u_2^h, v^h) &= -(g, v^h)_{0,\Gamma_0} + (T, v^h)_{0,\Omega_0} \quad \forall v^h \in V^h. \end{aligned}$$

Then we introduce a discrete cost functional

$$J_{r,\alpha}^h(T) = \frac{r}{2} \|u_1^h(T) - 2g\|_{0,\Gamma_0}^2 + \frac{1-r}{2} \|u_2^h(T) - 2g\|_{0,\Gamma_0}^2 + \frac{\alpha}{2} \|T\|_{0,\Omega_0}^2. \tag{23}$$

Problem 3.1: Find $S_{r,\alpha}^{h,H} \in Q_{ad}^H$ such that

$$J_{r,\alpha}^h(S_{r,\alpha}^{h,H}) = \inf_{T^H \in Q_{ad}^H} J_{r,\alpha}^h(T^H).$$

Results similar to Propositions 2.3 and 2.4 hold for Problem 3.1.

The solution $S_{r,\alpha}^{h,H}$ of Problem 3.1 is characterized by the inequality

$$\begin{aligned} \alpha(S_{r,\alpha}^{h,H}, T^H - S_{r,\alpha}^{h,H})_{0,\Omega_0} + r(u_1^h(S_{r,\alpha}^{h,H}) - 2g, u_1^h(T^H - S_{r,\alpha}^{h,H}))_{0,\Gamma_0} \\ + (1-r)(u_2^h(S_{r,\alpha}^{h,H}) - 2g, u_2^h(T^H) - u_2^h(S_{r,\alpha}^{h,H}))_{0,\Gamma_0} \geq 0 \quad \forall T^H \in Q_{ad}^H. \end{aligned} \tag{24}$$

We now provide a sample error bound for the approximate solution of Problem 2.2. For this purpose, assume $\Gamma \in C^{1,1}, D \in C^{0,1}, n \in C^{1,1}$ and $g \in L^2(\Gamma_0)$. Then for the solutions of the BVP (13) and (14), we have the regularity $u_1(T) \in H^2(\Omega)$ and $u_2(T) \in H^{3/2}(\Omega)$ [32]. The following error bounds are useful [12]: there exists a constant $c > 0$ independent of α, h and H such that for any $T \in Q$,

$$\begin{aligned} \|u_1^h(T) - u_1(T)\|_{0,\Omega} + h\|u_1^h(T) - u_1(T)\|_{1,\Omega} &\leq ch^2\|T\|_{0,\Omega_0}, \\ \|u_2^h(T) - u_2(T)\|_{0,\Omega} + h\|u_2^h(T) - u_2(T)\|_{1,\Omega} &\leq ch^{3/2}(\|g\|_{0,\Gamma_0} + \|T\|_{0,\Omega_0}). \end{aligned}$$

From these error bounds, together with the trace inequality $\|v\|_{0,\Gamma}^2 \leq c\|v\|_{0,\Omega}\|v\|_{1,\Omega}$ for any $v \in H^1(\Omega)$, we obtain

$$\|u_1^h(T) - u_1(T)\|_{0,\Gamma_0} \leq ch^{3/2}\|T\|_{0,\Omega_0} \quad \forall T \in Q \tag{25}$$

$$\|u_2^h(T) - u_2(T)\|_{0,\Gamma_0} \leq ch(\|g\|_{0,\Gamma_0} + \|T\|_{0,\Omega_0}) \quad \forall T \in Q. \tag{26}$$

Therefore, similar to the proof of Lemma 4.7 in [12], we have

$$\|u_1^h(\Pi^H T) - u_1(T)\|_{0,\Gamma_0} \leq cH\|T - \Pi^H T\|_{0,\Omega_0} + ch^{3/2}\|T\|_{0,\Omega_0} \quad \forall T \in Q \tag{27}$$

$$\|u_2^h(\Pi^H T) - u_2(T)\|_{0,\Gamma_0} \leq cH\|\Pi^H T - T\|_{0,\Omega_0} + ch(\|g\|_{0,\Gamma_0} + \|T\|_{0,\Omega_0}) \quad \forall T \in Q. \tag{28}$$

Downloaded By: [Gong, Rongfang] At: 05:01 20 March 2010

Denote

$$\begin{aligned}
 E_{r,\alpha}^{h,H} &= \alpha \|S_{r,\alpha} - S_{r,\alpha}^{h,H}\|_{0,\Omega_0}^2 + r \|u_1(S_{r,\alpha}) - u_1^h(S_{r,\alpha}^{h,H})\|_{0,\Gamma_0}^2 \\
 &\quad + (1-r) \|u_2(S_{r,\alpha}) - u_2^h(S_{r,\alpha}^{h,H})\|_{0,\Gamma_0}^2, \\
 E^H(S_{r,\alpha}) &= \|S_{r,\alpha} - \Pi^H S_{r,\alpha}\|_{0,\Omega_0} = \inf_{T^H \in Q_{ad}^H} \|S_{r,\alpha} - T^H\|_{0,\Omega_0}.
 \end{aligned}$$

Then we have the following error bound.

THEOREM 3.2 *There exists a constant $c > 0$ independent of α, r, h and H such that*

$$\begin{aligned}
 E_{r,\alpha}^{h,H} &\leq cr \|u_1(S_{r,\alpha}) - 2g\|_{0,\Gamma_0} (HE^H(S_{r,\alpha}) + h^{3/2} \|S_{r,\alpha}\|_{0,\Omega_0}) \\
 &\quad + cr (HE^H(S_{r,\alpha}) + h^{3/2} \|S_{r,\alpha}\|_{0,\Omega_0})^2 \\
 &\quad + c(1-r) \|u_2(S_{r,\alpha}) - 2g\|_{0,\Gamma_0} (HE^H(S_{r,\alpha}) + h \|S_{r,\alpha}\|_{0,\Omega_0}) \\
 &\quad + c(1-r) (HE^H(S_{r,\alpha}) + h \|S_{r,\alpha}\|_{0,\Omega_0})^2.
 \end{aligned} \tag{29}$$

Proof Substitute $T = S_{r,\alpha}^{h,H}$ in (18), $T^H = \Pi^H S_{r,\alpha}$ in (24), and add the two resulting inequalities to obtain

$$\begin{aligned}
 E_{\alpha}^{h,H} &\leq \alpha (S_{r,\alpha}^{h,H}, \Pi^H S_{r,\alpha} - S_{r,\alpha})_{0,\Omega_0} \\
 &\quad + r (u_1(S_{r,\alpha}) - 2g, u_1^h(\Pi^H S_{r,\alpha}) - u_1(S_{r,\alpha}))_{0,\Gamma_0} \\
 &\quad + r (u_1(S_{r,\alpha}) - u_1^h(S_{r,\alpha}^{h,H}), u_1(S_{r,\alpha}) - u_1^h(\Pi^H S_{r,\alpha}))_{0,\Gamma_0} \\
 &\quad + (1-r) (u_2(S_{r,\alpha}) - 2g, u_2^h(\Pi^H S_{r,\alpha}) - u_2(S_{r,\alpha}))_{0,\Gamma_0} \\
 &\quad + (1-r) (u_2(S_{r,\alpha}) - u_2^h(S_{r,\alpha}^{h,H}), u_2(S_{r,\alpha}) - u_2^h(\Pi^H S_{r,\alpha}))_{0,\Gamma_0} \\
 &\leq \alpha (S_{r,\alpha}^{h,H}, \Pi^H S_{r,\alpha} - S_{r,\alpha})_{0,\Omega_0} \\
 &\quad + r \|u_1(S_{r,\alpha}) - 2g\|_{0,\Gamma_0} \|u_1^h(\Pi^H S_{r,\alpha}) - u_1(S_{r,\alpha})\|_{0,\Gamma_0} \\
 &\quad + \frac{r}{2} \|u_1(S_{r,\alpha}) - u_1^h(S_{r,\alpha}^{h,H})\|_{0,\Gamma_0}^2 + \frac{r}{2} \|u_1(S_{r,\alpha}) - u_1^h(\Pi^H S_{r,\alpha})\|_{0,\Gamma_0}^2 \\
 &\quad + (1-r) \|u_2(S_{r,\alpha}) - 2g\|_{0,\Gamma_0} \|u_2^h(\Pi^H S_{r,\alpha}) - u_2(S_{r,\alpha})\|_{0,\Gamma_0} \\
 &\quad + \frac{1-r}{2} \|u_2(S_{r,\alpha}) - u_2^h(S_{r,\alpha}^{h,H})\|_{0,\Gamma_0}^2 + \frac{1-r}{2} \|u_2(S_{r,\alpha}) - u_2^h(\Pi^H S_{r,\alpha})\|_{0,\Gamma_0}^2.
 \end{aligned}$$

Applying (22), (27) and (28), we obtain (29). ■

Under additional assumptions, we can deduce more concrete error bounds from Theorem 3.2. For instance, if Q_{ad} is a bounded set in the space Q , then there is a constant $c > 0$ independent of α, h and H such that

$$E_{\alpha}^{h,H} \leq c H E^H(S_{r,\alpha}) + cr h^{3/2} + c(1-r)h.$$

We note that as we have seen in Section 3 that with proper choice of α related to h and H , we can show the convergence of $S_{r,\alpha}^{h,H}$ to $S_{r,*}$ as $h, H, \alpha \rightarrow 0^+$, assuming that S_r is nonempty, where $S_{r,*}$ has minimal L^2 -norm among the solution set of Problem 2.2 with $\alpha = 0$.

4. Numerical experiments

In this section, we will show some simulation results. We limit ourselves to the two-dimensional case.

Downloaded By: [Gong, Rongfang] At: 05:01 20 March 2010

4.1. Implementation detail

Let $\varphi_i(x) \in V^h$ be the nodal basis functions of the finite element space V^h associated with the grid nodes $x_i, i = 1, 2, \dots, N$ (N is the number of nodes of the triangulation \mathcal{T}_h). Then, $u_1^h = \sum_{i=1}^N u_i^{(1)} \varphi_i, u_2^h = \sum_{i=1}^N u_i^{(2)} \varphi_i$, with $u_i^{(1)} = u_1^h(x_i)$ and $u_i^{(2)} = u_2^h(x_i)$, respectively. Denote triangulation $\mathcal{T}_{0,H} = \{K_{0,l}\}, l = 1, 2, \dots, N_0$ (N_0 is the number of elements of triangulation $\mathcal{T}_{0,H}$), that is, $\overline{\Omega_0} = \bigcup_{l=1}^{N_0} K_{0,l}$, then an approximate light source $S^H \in Q^H$ has form $S^H|_{K_{0,l}} = s_{0,l}$ with $s_{0,l} \geq 0, l = 1, 2, \dots, N_0$. Assume that $\mathcal{T}_{0,H}$ and \mathcal{T}_h are consistent, that is, $\mathcal{T}_{0,H}$ can be viewed as a restriction of the triangulation \mathcal{T}_h on $\overline{\Omega_0}$. We further let the end points of Γ_0 be grid points of the triangulation \mathcal{T}_h . For the ease of our statement, denote $I = \{1, 2, \dots, N\}, I_0 = \{1, 2, \dots, N_0\}, I_b = \{i \in I | x_i \in \Gamma\}, I_b^0 = \{i \in I | x_i \in \overline{\Gamma_0}\} = \{b_1, b_2, \dots, b_{N_b^0}\}$ with $b_1 < b_2 < \dots < b_{N_b^0}$ and N_b^0 the number of the grid nodes on the boundary $\overline{\Gamma_0}$, and $I_b^1 = \{i \in I | x_i \in \overline{\Gamma_1}\}$ with N_b^1 the number of the grid nodes on the boundary $\overline{\Gamma_1}$. Moreover, define

$$\begin{aligned}
 A &= (a_{ij})_{N \times N}, & a_{ij} &= \int_{\Omega} D \nabla \varphi_j \cdot \nabla \varphi_i dx, \quad i, j \in I, \\
 B &= (b_{ij})_{N \times N}, & b_{ij} &= - \int_{\Omega} D \frac{2\varphi_j}{n} \nabla n \cdot \nabla \varphi_i dx, \quad i, j \in I, \\
 C &= (c_{ij})_{N \times N}, & c_{ij} &= \int_{\Omega} \mu_a \varphi_j \varphi_i dx, \quad i, j \in I, \\
 E &= (e_{ij})_{N \times N}, & e_{ij} &= \begin{cases} \frac{1}{2} \int_{\Gamma} \varphi_j \varphi_i d\sigma, & i, j \in I_b, \\ 0, & \text{otherwise,} \end{cases} \\
 E^0 &= (e_{ij}^0)_{N \times N_b^0}, & e_{ij}^0 &= \begin{cases} \frac{1}{2} \int_{\Gamma_0} \varphi_j \varphi_i d\sigma, & i, j \in I_b^0, \\ 0, & j \in I_b^0, i \in I \setminus I_b^0, \end{cases} \\
 E^1 &= (e_{ij}^1)_{N \times N}, & e_{ij}^1 &= \begin{cases} \frac{1}{2} \int_{\Gamma_1} \varphi_j \varphi_i d\sigma, & i, j \in I_b^1, \\ 0, & \text{otherwise,} \end{cases} \\
 R &= (r_{ij})_{N \times N_0}, & r_{ij} &= \begin{cases} \int_{K_{0,j}} \varphi_i dx, & i \in I_j, j \in I_0, \\ 0, & i \in I \setminus I_j, j \in I_0, \end{cases}
 \end{aligned}$$

where $I_j = \{i \in I | \widehat{K}_i \cap K_{0,j} \neq \emptyset\}$ and \widehat{K}_i is the support of the basis function φ_i . We further denote by $U^{(1)}$ and $U^{(2)}$ the vectors $(u_1^{(1)}, u_2^{(1)}, \dots, u_N^{(1)})^t$ and $(u_1^{(2)}, u_2^{(2)}, \dots, u_N^{(2)})^t$, respectively, and again by S the vector $(s_1, s_2, \dots, s_{N_0})^t$, where a superscript t stands for transposition. For numerical simulation, b_{ij} is computed as follows.

$$\begin{aligned}
 b_{ij} &= - \int_{\Omega} D \frac{2 \nabla n}{n} \varphi_j \nabla \varphi_i dx = - \sum_{K \in \mathcal{T}_h} \int_K D \frac{2 \nabla n}{n} \varphi_j \nabla \varphi_i dx \\
 &= - \sum_{K \in \mathcal{T}_h} \left(\frac{\nabla n}{n} \right)_{G_K} \int_K 2 D \varphi_j \nabla \varphi_i dx.
 \end{aligned}$$

Here $(\rho(x))_{G_K}$ denotes the value of function ρ at the gravitational centre of the triangle K . To obtain the representation of matrix form, we let

$$\begin{aligned}
 L^1 &= A + B + C + E, & F^1 &= RS, \\
 L^2 &= A + B + C + E^1, & F^2 &= E^0 g + F^1,
 \end{aligned}$$

Downloaded By: [Gong, Rongfang] At: 05:01 20 March 2010

where we use the same symbol g for the function $g(x)$ and the vector $g = (g_1, g_2, \dots, g_{N_b^0})^t$ with $g_i = g(x_{b_i}), i = 1, 2, \dots, N_b^0$. Then we have the systems

$$L^k U^{(k)} = F^k, \quad k = 1, 2. \tag{30}$$

We can solve the linear system (30) with any fast methods including direct and iterative methods. In our experiments, we use direct method when the system size is relatively small and use bi-conjugate gradient method (BiCG) [33] when the system size is large. Consequently, the functional $J_{r,\alpha}^h(S^h)$ reduces to

$$\begin{aligned} J_{r,\alpha}^h(S^h) &= \frac{\alpha}{2} \sum_{l=1}^{N_0} s_l^2 |K_{0,l}| + \frac{r}{2} \int_{\Gamma_0} \left(\sum_{i \in I_b^0} u_i^{(1)} \varphi_i - 2g \right)^2 d\sigma \\ &\quad + \frac{1-r}{2} \int_{\Gamma_0} \left(\sum_{i \in I_b^0} u_i^{(2)} \varphi_i - 2g \right)^2 d\sigma, \end{aligned}$$

where $|K_{0,l}|$ is the area of the element $K_{0,l}$.

Define $V_{\Gamma_0}^h = \{v|_{\Gamma_0} \mid v \in V^h\} \subset L^2(\Gamma_0)$, which is spanned by $\{\varphi_i|_{\Gamma_0}\}_{i \in I_b^0}$. Express the solutions $U^{(k)}$ ($k = 1, 2$) of the linear systems (30) as $U^{(1)} = M^1 S$ and $U^{(2)} = \eta + M^2 S$ with $M^k = (m_{ij}^k)_{N \times N_0}$ and η a vector of N components. Let

$$\begin{aligned} \eta^0 &= (\eta_i^0)_{N_b^0 \times 1}, \quad \eta_i^0 = \eta(b_i), \quad i = 1, 2, \dots, N_b^0, \\ E^{00} &= (e_{ij}^{00})_{N_b^0 \times N_b^0}, \quad e_{ij}^{00} = E^0(b_i, j), \quad i, j = 1, 2, \dots, N_b^0, \\ M^{k0} &= (m_{ij}^{k0})_{N_b^0 \times N_0}, \quad m_{ij}^{k0} = M^k(b_i, j), \quad i = 1, 2, \dots, N_b^0, j \in I_0, k = 1, 2. \end{aligned}$$

We further have

$$\begin{aligned} f(S) &\equiv J_{r,\alpha}^h(S^h) \\ &= \frac{\alpha}{2} \sum_{l=1}^{N_0} s_l^2 |K_{0,l}| + \frac{r}{2} \int_{\Gamma_0} \left(\sum_{i \in I_b^0} u_i^{(1)} \varphi_i - 2g \right)^2 d\sigma \\ &\quad + \frac{1-r}{2} \int_{\Gamma_0} \left(\sum_{i \in I_b^0} u_i^{(2)} \varphi_i - 2g \right)^2 d\sigma \\ &= \frac{\alpha}{2} \sum_{l=1}^{N_0} s_l^2 |K_{0,l}| + \frac{r}{2} \int_{\Gamma_0} \left[\sum_{i=1}^{N_b^0} \left(\sum_{j=1}^{N_0} m_{bj}^1 s_j - 2g_i \right) \varphi_{b_i} \right]^2 d\sigma \\ &\quad + \frac{1-r}{2} \int_{\Gamma_0} \left[\sum_{i=1}^{N_b^0} \left(\sum_{j=1}^{N_0} m_{bj}^2 s_j + \eta_{b_i} - 2g_i \right) \varphi_{b_i} \right]^2 d\sigma \\ &= \frac{\alpha}{2} S^t \text{diag}(|K_{0,1}|, |K_{0,2}|, \dots, |K_{0,N_0}|) S + \frac{r}{2} (M^{10} S - 2g)^t E^{00} (M^{10} S - 2g) \\ &\quad + \frac{1-r}{2} (M^{20} S + \eta^0 - 2g)^t E^{00} (M^{20} S + \eta^0 - 2g). \end{aligned}$$

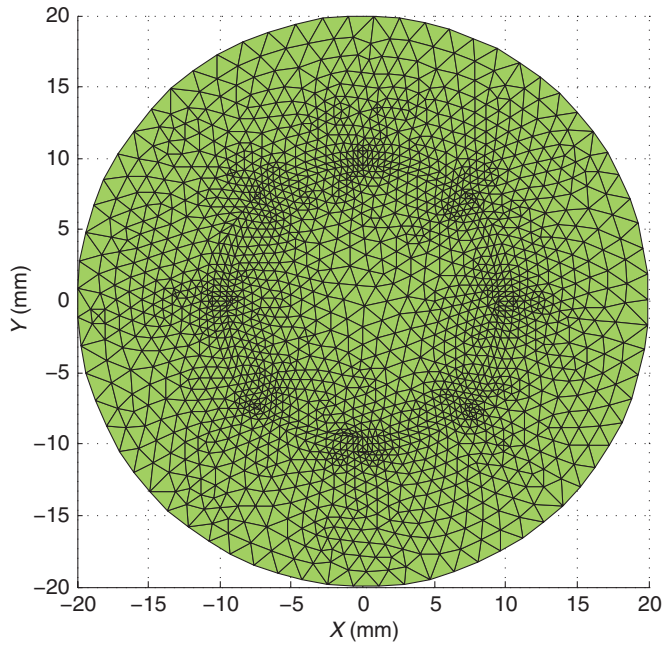


Figure 1. Triangulation of $\bar{\Omega}$ for a single light source problem.

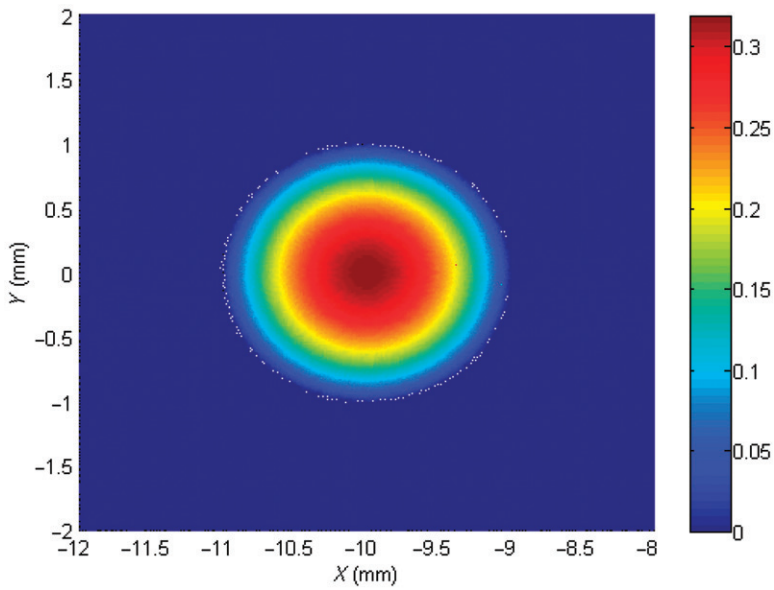
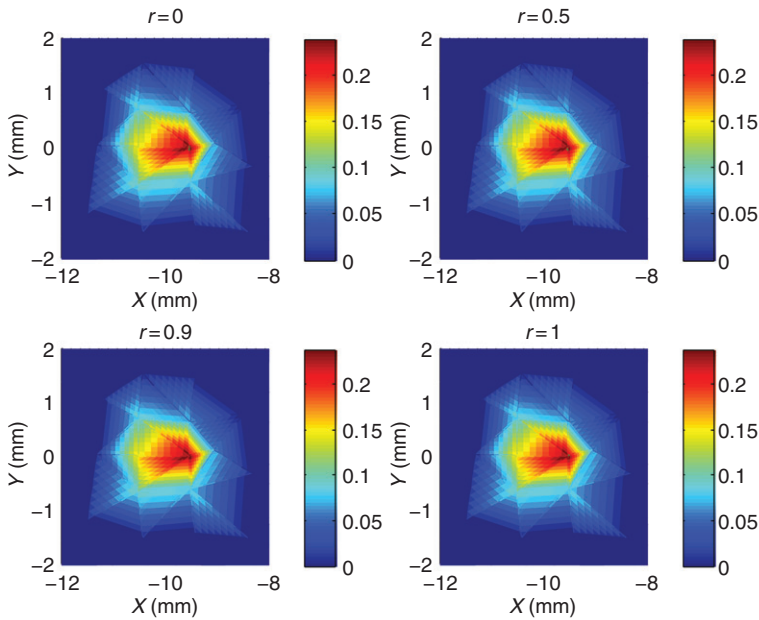


Figure 2. (Available in colour online). Exact single light source.

Table 1. Error $\|S_{r,\alpha}^{h,h} - S\|_Q$ for different parameter r .

r	$NT=968, N=502$	$NT=3872, N=1971$	$NT=15,488, N=7813$
0	$1.32667e-3$	$1.21078e-3$	$1.14923e-3$
0.1	$1.32654e-3$	$1.21022e-3$	$6.84920e-4$
0.3	$1.32644e-3$	$1.20880e-3$	$1.12576e-3$
0.5	$1.32634e-3$	$1.20844e-3$	$1.07552e-3$
0.7	$1.32619e-3$	$1.20680e-3$	$1.15209e-3$
0.9	$1.32607e-3$	$1.20620e-3$	$1.15432e-3$
0.99	$1.32600e-3$	$1.20596e-3$	$1.15331e-3$
0.999	$1.32600e-3$	$1.20511e-3$	$1.15330e-3$
1	$1.32600e-3$	$1.20553e-3$	$1.15330e-3$

Figure 3. (Available in colour online). Reconstructed single light source with $NT = 968, N = 502$ for $r = 0, r = 0.5, r = 0.9$ and $r = 1$.

Then Problem 3.1 reduces to the following quadratic programming problem:

$$\min_{S \in \mathbb{R}^{N_0}, S \geq 0} f(S). \quad (31)$$

4.2. Numerical results

In our simulations, the problem domain $\Omega \subset \mathbb{R}^2$ is a circle centred at the origin with radius 20 mm, the reduced scattering coefficient $\mu'_s = 1.0$, the absorption coefficient $\mu_a = 0.020$, and the refractive index

$$n(x, y) = 1 + 0.5 \times 10^{-0.01 \min\{10.5^2, \max\{x^2 + y^2, 9.5^2\}\}}.$$

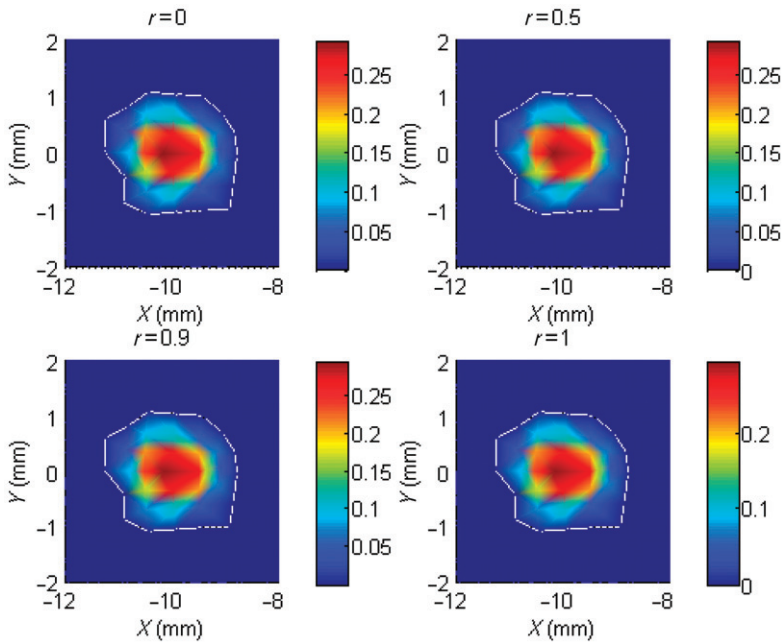


Figure 4. (Available in colour online). Reconstructed single light source with $NT = 3872$, $N = 1971$ for $r=0$, $r=0.5$, $r=0.9$ and $r=1$.

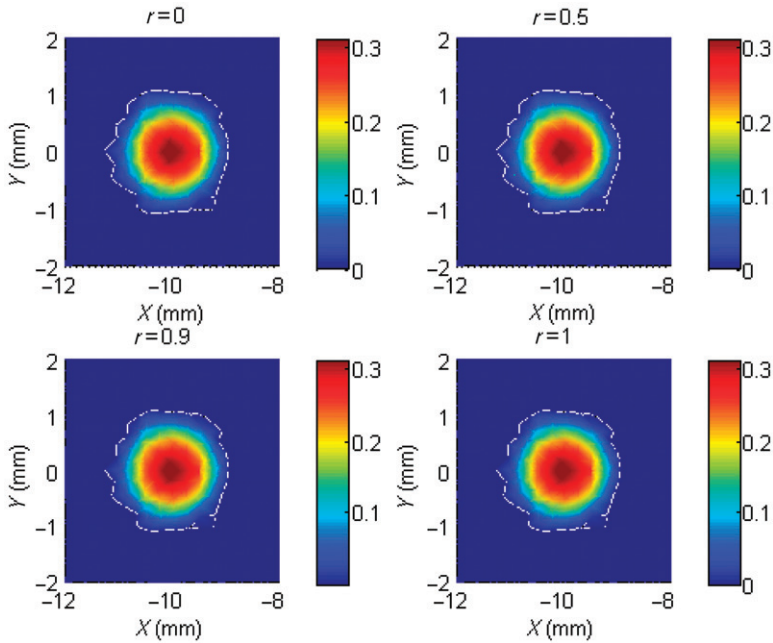


Figure 5. (Available in colour online). Reconstructed single light source with $NT = 15488$, $N = 7813$ for $r=0$, $r=0.5$, $r=0.9$ and $r=1$.

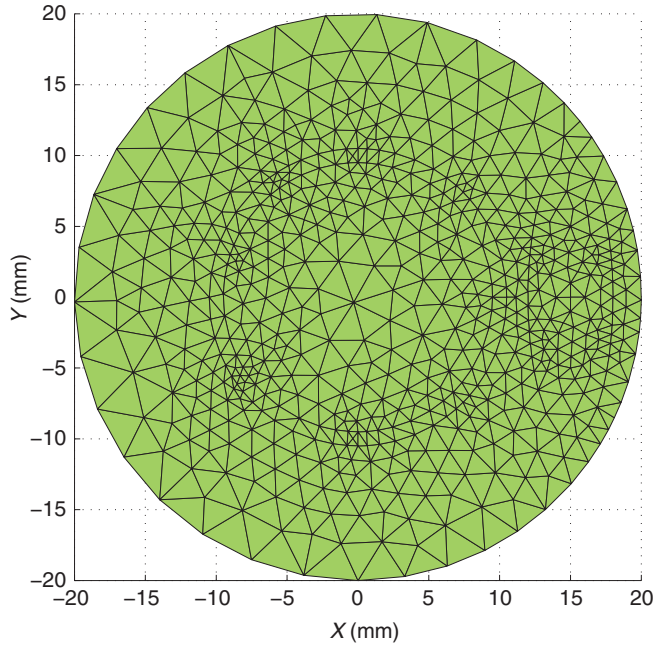


Figure 6. Triangulation of $\bar{\Omega}$ for a multiple light source problem.

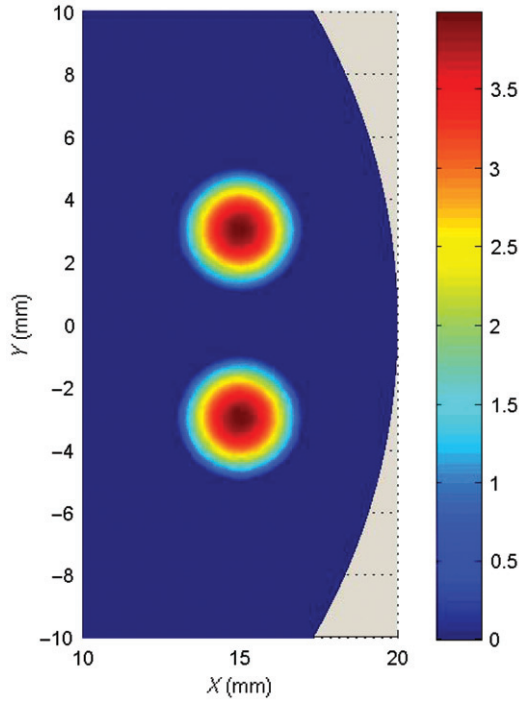


Figure 7. (Available in colour online). Exact multiple light source.

Downloaded By: [Gong, Rongfang] At: 05:01 20 March 2010

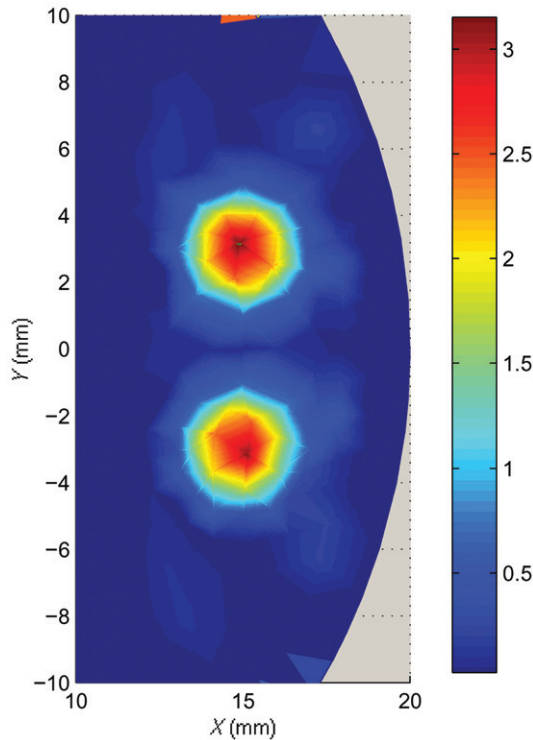


Figure 8. (Available in colour online). Reconstructed multiple light source with 1225 elements and 637 nodes, $r = 1$.

With a given permissible region Ω_0 , we use $Q_{ad} = \{S \in Q \mid S \geq 0 \text{ a.e. in } \Omega_0\}$ for the admissible set of the light source function. We assume that the observations are available on part of the boundary $\Gamma_0 = \{(x, y) \mid x^2 + y^2 = 20^2; x \geq 0\}$, the measurement g on Γ_0 is polluted by noise with level 10%, and the Tikhonov regularization parameter $\alpha = 1 \times 10^{-5}$. We use Delaunay elements for the triangulations. For a triangulation, denote by NT and N the numbers of elements and nodes.

We first consider a single light source reconstruction problem. A light source of density $S(x, y) = (1 - (x + 10)^2 - y^2)/\pi$ is placed on a circle centred at $(-10, 0)$ with radius 1 mm. Let the permissible region $\Omega_0 = \{(x, y) \mid (x + 10)^2 + y^2 < 2^2\}$. We show the triangulation and the exact light source function S in Figures 1 and 2. Figures 3–5 show approximate light source $S_\alpha^{h,h}$ for partition with NT=968, N=502, NT=3872, N=1971 and NT=15488, N=7813, respectively. Each figure contains four pictures corresponding to $r=0$, $r=0.5$, $r=0.9$ and $r=1$. We conclude from these figures that the smaller the meshsize is, the better the light source reconstruction.

To see the influence of the parameter r on the accuracy of the numerical solution, we report in Table 1 the numerical solution errors for several choices of the parameter. It can be seen from Table 1 that for a fixed triangulation, error in approximate light source gets smaller slightly when the parameter becomes bigger until near $r = 1$. We also observe that it is possible to adjust the value of the parameter r so as to achieve better accuracy of the approximate light source function than the conventional formulation ($r = 1$, corresponding to a single forward boundary value problem). How to determine an optimal value for the

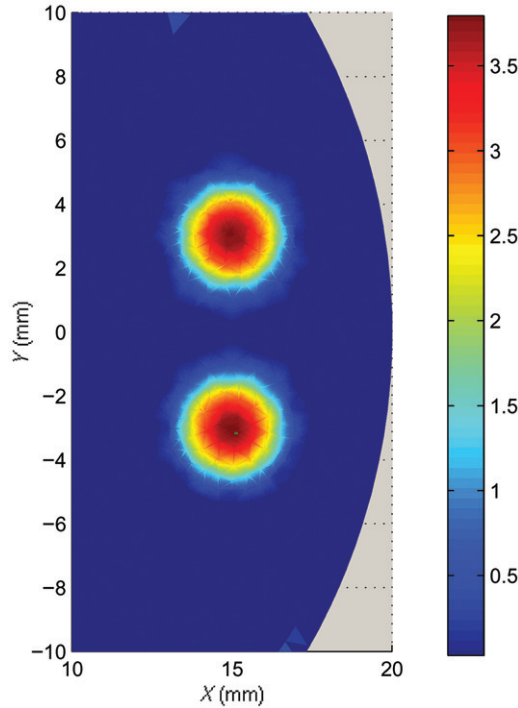


Figure 9. (Available in colour online). Reconstructed multiple light source with 4900 elements and 2498 nodes, $r = 1$.

parameter r is a topic worth further investigation. The numerical results also suggest that generally the conventional choice $r = 1$ is quite satisfactory.

We then consider a reconstruction problem with two distinguish light sources. Place two circular light sources with radius 2 mm at $(15, 3)$ and $(15, -3)$, with densities $4 - (x - 15)^2 - (y - 3)^2$ and $4 - (x - 15)^2 - (y + 3)^2$, respectively. We choose the permissible region $\Omega_0 = \{(x, y) \mid (x - 15)^2/9 + y^2/100 < 1\}$. The triangulation and the exact light source function are plotted in Figures 6 and 7. Reconstructed light source functions are shown in Figures 8 and 9 with partition of 1225 triangle elements and 637 nodes, and partition of 4900 triangle elements and 2498 nodes respectively.

We observe that in all our numerical simulations, the light source functions are well reconstructed.

Acknowledgements

This work was supported by the National Science Foundation of China under Grant No. 10871179 and the National Basic Research Programme of China under Grant No. 2008CB717806.

References

- [1] A. Douraghy, D.L. Prout, R.W. Silverman, and A.F. Chatzioannou, *Evaluation of scintillator afterglow for use in a combined optical and PET imaging tomography*, Nucl. Instr. Meth. A 569 (2006), pp. 557–562.

- [2] W.T. Loo, J.M. Tong, M.N. Cheung, and L.W. Chow, *A new predictive and prognostic marker (ATP bioluminescence and positron emission tomography) in vivo and in vitro for delivering adjuvant treatment plan to invasive breast tumor patients*, Biomed. Pharmacother. 60 (2006), pp. 285–288.
- [3] G. Genove, U. DeMarco, H. Xu, W.F. Goins, and E.T. Ahrens, *A new transgene reporter for in vivo magnetic resonance imaging*, Nat. Med. 11 (2005), pp. 450–454.
- [4] R. Weissleder and V. Ntziachristos, *Shedding light onto live molecular targets*, Nat. Med. 9 (2003), pp. 123–128.
- [5] D. Boas, D.H. Brooks, E.L. Miller, C.A. DiMarzio, M. Kilmer, R.J. Gaudette, and Q. Zhang, *Imaging the body with diffuse optical tomography*, IEEE Signal Process. Mag. 18 (2001), pp. 57–75.
- [6] W.X. Cong, D. Kumar, Y. Liu, A. Cong, and G. Wang, *A practical method to determine the light source distribution in bioluminescent imaging*, Proc. SPIE 5535 (2004), pp. 679–686.
- [7] X. Gu, Q. Zhang, L. Larcom, and H. Jiang, *Three dimensional bioluminescence tomography with model-based reconstruction*, Opt. Express 12 (2004), pp. 3996–4000.
- [8] G. Alexandrakis, F.R. Rannou, and A.F. Chatzioannou, *Tomographic bioluminescence imaging by use of a combined optical-PET (OPET) system: A computer simulation feasibility study*, Phys. Med. Biol. 50 (2005), pp. 4225–4241.
- [9] A.J. Chaudari, F. Darvas, J.R. Bading, R.A. Moats, P.S. Conti, D.J. Smith, S.R. Cherry, and R.M. Leahy, *Hyperspectral and multispectral bioluminescence optical tomography for small animal imaging*, Phys. Med. Biol. 50 (2005), pp. 5421–5441.
- [10] X.-L. Cheng, R.-F. Gong, and W. Han, *A new general mathematical framework for bioluminescence tomography*, Comput. Methods Appl. Mech. Eng. 197 (2008), pp. 524–535.
- [11] W.X. Cong, K. Durairaj, L.V. Wang, and G. Wang, *A Born-type approximation method for bioluminescence tomography*, Med. Phys. 33 (2006), pp. 679–686.
- [12] W. Han, W.X. Cong, and G. Wang, *Mathematical theory and numerical analysis of bioluminescence tomography*, Inverse Probl. 22 (2006), pp. 1659–1675.
- [13] W. Han, W.X. Cong, and G. Wang, *Mathematical study and numerical simulation of multispectral bioluminescence tomography*, Int. J. Biomed. Imag. 2006 (2006), Article ID 54390.
- [14] W. Han and G. Wang, *Theoretical and numerical analysis on multispectral bioluminescence tomography*, IMA J. Appl. Math. 72 (2007), pp. 67–85.
- [15] K. Kwon, B. Yazici, and M. Guven, *Two-level domain decomposition methods for diffuse optical tomography*, Inverse Probl. 22 (2006), pp. 1533–1559.
- [16] N.V. Slavine, M.A. Lewis, E. Richer, and P.P. Antich, *Iterative reconstruction method for light emitting sources based on the diffusion equation*, Med. Phys. 33 (2006), pp. 61–69.
- [17] H. Li, J. Tian, F. Zhu, W.X. Cong, L.V. Wang, E.A. Hoffman, and G. Wang, *A mouse optical simulation environment (MOSE) to investigate bioluminescent phenomena in the living mouse with the Monte Carlo method*, Acad. Radiol. 11 (2004), pp. 1029–1038.
- [18] F. Natterer and F. Wübbeling, *Mathematical Methods in Image Reconstruction*, SIAM Monographs on Mathematical Modeling and Computation, SIAM, Philadelphia, PA, 2001.
- [19] E. Acosta and D. Vazquez, *Tomographic method for measurement of the gradient refractive index of the crystalline lens I: The spherical fish lens*, J. Opt. Soc. Am. A 22 (2005), pp. 424–433.
- [20] N. Barakat, H.A. El-Hennawi, H. El-Ghandoor, R. Hassan, and F. El-Diasty, *Three-dimensional refractive index profile of a HRIN optical waveguide using multiple beam interference fringes*, Opt. Commun. 191 (2001), pp. 39–47.
- [21] H.A. Ferwerda, *The radiative transfer equation for scattering media with spatially varying refractive index*, J. Opt. A: Pure Appl. Opt. 1 (1999), pp. L1–2.
- [22] T. Khan and H. Jiang, *A new diffusion approximation to the radiative transfer equation for scattering media with spatially varying refractive indices*, J. Opt. A: Pure Appl. Opt. 5 (2003), pp. 137–141.

- [23] T. Khan and A. Thomas, *Comparison of P_N or spherical harmonics approximation for scattering media with spatially varying and spatially constant refractive indices*, *Opt. Commun.* 255 (2005), pp. 130–166.
- [24] M.L. Shendeleva, *Radiative transfer in a turbid medium with a varying refractive index: Comment*, *J. Opt. Soc. Am. A* 21 (2004), pp. 2464–2467.
- [25] J.M. Tualle and E. Tinet, *Derivation of the radiative transfer equation for scattering media with a spatially varying refractive index*, *Opt. Commun.* 228 (2003), pp. 33–38.
- [26] T. Khan and A. Thomas, *Inverse problem in refractive index based optical tomography*, *Inverse Probl.* 22 (2006), pp. 1121–1137.
- [27] T. Khan, A. Thomas, and J.R. Yoon, *On uniqueness in refractive index optical tomography*, *Inverse Probl.* 22 (2006), pp. L1–L5.
- [28] K. Atkinson and W. Han, *Theoretical Numerical Analysis: A Functional Analysis Framework*, 2nd ed., Springer-Verlag, New York, 2005.
- [29] J.N. Franklin, *On Tikhonov's method for ill-posed problems*, *Math. Comp.* 28 (1974), pp. 889–907.
- [30] V. Isakov, *Inverse Problems for Partial Differential Equations*, 2nd ed., Springer, New York, 2006.
- [31] A. Kirsch, *An Introduction to the Mathematical Theory of Inverse Problems*, Applied Mathematical Sciences, Vol. 120, Springer-Verlag, New York, 1996.
- [32] P. Grisvard, *Elliptic Problems in Nonsmooth Domains*, Pitman, Boston, 1985.
- [33] Y. Saad, *Iterative Methods for Sparse Linear Systems*, 2nd ed., SIAM, Philadelphia, 2003.